Results in Engineering 24 (2024) 103343

Contents lists available at ScienceDirect

Results in Engineering

journal homepage: www.sciencedirect.com/journal/results-in-engineering

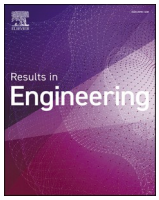

Novel biolubricant synthesis: Enhancing the composition of used cooking oil and *Callophyllum inophyllum* oil by utilizing infrared heating method

Bela Nurulita [a,c], Taufiq Bin Nur [a], Arridina Susan Silitonga [b,c,*], Teuku Meurah Indra Riayatsyah [b], Deswita [e], Md Abul Kalam [b], Nurin Wahidah Mohd Zulkifli [d], Abdi Hanra Sebayang [c], Sihar Siahaan [c], Munawar Alfansury [f]

[a] *Department of Mechanical Engineering, University of Sumatera Utara, Padang Bulan, Medan, 20155, Indonesia*
[b] *Centre for Technology in Water and Wastewater, School of Civil and Environmental Engineering, Faculty of Engineering and Information Technology, University of Technology Sydney, NSW, 2007, Australia*
[c] *Center of Renewable Energy, Department of Mechanical Engineering, Politeknik Negeri Medan, 20155, Medan, Indonesia*
[d] *Department of Mechanical Engineering, Faculty of Engineering, University of Malaya, Kuala Lumpur, 50603, Malaysia*
[e] *National Innovation and Research Agency, BRIN Kawasan Puspiptek, Serpong, Tangerang, Banten, 15314, Indonesia*
[f] *Department of Mechanical Engineering, Faculty of Engineering, Universitas Muhammadiyah Sumatera Utara, 20238, Medan, Indonesia*

ARTICLE INFO

Keywords:
Biolubricant synthesis
Crude oil blend
Infrared heating
Response surface methodology
Physicochemical properties
Tribological characteristics

ABSTRACT

This study presents a novel biolubricant synthesis method using infrared heating to produce biolubricant from a blend of used cooking oil and *Calophyllum inophyllum* oil (UCOCI). Response Surface Methodology was applied to optimize the polyesterification process, varying reaction time, ethylene glycol (EG) to UCOCI methyl ester ratio, and sodium methoxide concentration. The predicted biolubricant yield was 94.30 %, closely matching the experimental yield of 94.03 %. The quadratic response model demonstrated a strong fit ($R^2 = 0.9979$). Physicochemical and tribological properties were evaluated and compared to SAE 15-W40 lubricant. UCOCI biolubricant showed an acid value of 0.46 mg KOH/g, viscosities of 83.46 cSt at 40 °C and 13.2 cSt at 100 °C, and a viscosity index of 216.32. Friction coefficients of UCOCI biolubricant blends (Biol10 to Biol50) ranged from 0.1091 to 0.071, all lower than SAE 15W-40. The wear scar diameters for these blends (0.140 to 0.100 mm) were also significantly smaller than SAE 15W-40 (0.549 mm). The superior lubricating properties suggest UCOCI biolubricant's potential for use in heavy-duty engines and as a natural additive.

1. Introduction

Today's primary global energy comes from fossil fuels that gradually replete and will soon be exhausted. According to statistical data from the Energy Institute, 81.47 % of the global energy is derived from fossil fuels and while 18.53 % is derived from renewable sources [1]. In Indonesia, 87.7 % of fossil fuel energy constitutes the total primary energy sources in 2021, where the fossil fuel energy is dominated by coal (42.38 %), followed by petroleum (31.40 %), and natural gas (13.92 %) [2]. Increasing the use of fossil fuels will increase local and global air pollution and exacerbate the issue of global warming due to release of carbon dioxide emissions (CO_2) into the atmosphere. Moreover, the global energy crisis, marked by rising oil prices, has prompted scholars and the industry to shift their energy sources to more environmentally friendly, renewable, and sustainable energy sources. One of the forms of alternative energy that is extensively studied and developed is biolubricants.

Biolubricants are derived from renewable sources (including vegetable oils and animal fats), serving as alternative lubricants and superior substitutes or additives for conventional petroleum-derived lubricants [3–6]. Biolubricants are an excellent alternative to conventional petroleum-derived lubricants. The consumption of the global lubricant industry is projected to significantly increase, reaching a compound annual growth rate (CAGR) of 3.8 %, from USD 139.44 billion in 2023 to USD 180.21 billion by 2030 [7]. Every year, 40 million metric tonnes of lubricant are produced worldwide, and about half of that is discharged into the environment, with devastating impacts on the environment such as water and soil pollution [8,9].

The disposal of commercial lubricants is detrimental to the environment, and therefore, many scholars are exploring environmentally

* Corresponding author.
E-mail address: ardinsu@yahoo.co.id (A.S. Silitonga).

https://doi.org/10.1016/j.rineng.2024.103343
Received 15 September 2024; Received in revised form 20 October 2024; Accepted 5 November 2024
Available online 7 November 2024

friendly biolubricant raw materials such as inedible raw materials [10,11], including used cooking oil (UCO) [6,12], *Calophyllum inophyllum* oil (CIO) [13], *Jatropha curcas* oil [14], rubber seed oil [15], and kapok oil [9]. The use of edible oils such as crude coconut oil for biolubricant production will increase the price of the crude oil owing to the competition between the use of edible oils for food and lubricant production [16]. Consequently, the cost of biolubricant production will increase by a factor of 4–15 compared with the cost of conventional mineral lubricant production [17].

In the commercialization of biodiesels and biolubricants, the main problem is the price of raw materials, especially vegetable oils [18]. Therefore, the production of biolubricant from used cooking oil (UCO) is a cost-effective option, which can also address the problem of UCO disposal. From 2023 to 2030, the compound annual growth rate (CAGR) is projected at 4.8 %, with the global UCO market anticipated to increase from USD 7.29 billion in 2022 to USD 10.61 billion by 2030 [19]. In 2023, Indonesia's palm oil production was estimated at approximately 46.98 million metric tonnes, showing a consistent upward trend. The production saw a significant growth of 7.15 % from the previous year, which was attributed to favourable weather conditions and an expansion of plantation areas. The high potential of palm oil in Indonesia produces large amounts of UCO that can be potentially used as a raw material for biolubricants. Converting UCOs into biolubricants or other bioproducts will not only reduce the adverse impacts of UCO on the environment, but it will also prevent illegal UCO recycling as fake palm oil [17,20]

UCO has poor oxidation stability and low viscosity, necessitating further research to improve its physicochemical properties [21]. The kinematic viscosity and oxidation stability are important properties of lubricants [22]. Different oil blends have been investigated for biodiesel production and it has been shown that the type of oil blend plays an important role in improving the physicochemical properties of the biodiesel such as kinematic viscosity and oxidation stability [22]. CIO is one of the inedible raw materials that can improve the physicochemical properties of UCO. Based on gas chromatography–mass spectrometry measurements, CIO contains stearate acid (43.33 %) and linoleic acid (31.18 %). The total saturated and unsaturated fatty acids are 58.77 and 41.24 %, respectively [23]. Based on its fatty acid composition, it is expected that CIO is capable of enhancing the physicochemical properties when it is blended with UCO.

It is essential to evaluate biolubricant production technology to reduce production costs. Various methods have been used to synthesize biolubricants such as conventional [6,24], microwave [25–27], ultrasound [28,29], and supercritical fluid [30] methods. Numerous studies have reported that the transesterification of vegetable oil triester with trimethylolpropane (TMP), neopentyl glycol (NPG), ethylene glycol (EG), and pentaerythritol (PET) as polyols to produce biolubricants using conventional reactors requires 4–6 h [5,10,25,31–34]. This is important because long reaction times translate to higher energy consumption and production costs. The intensification process is a chemical process that is more sustainable, improves performance, and reduces costs [28]. Infrared heating is one of the most efficient methods to intensify chemical reactions [35]. In an infrared irradiation-assisted reactor with an infrared energy within a range of 0.001–1.7 eV, the infrared radiation can penetrate deeper into the reaction mass and be intensively absorbed [20].

However, to date, there are limited reports on the synthesis of biolubricant from a blend of UCO and CIO using infrared irradiation-assisted reactor. The objective of this study is to produce high-quality UCOCI biolubricant using this novel synthesis method and characterize its physicochemical properties and tribological characteristics. Furthermore, the process variables of the UCOCI biolubricant production process assisted by infrared irradiation was optimized using response surface methodology (RSM) based on the Box–Behnken design. RSM is an empirical model that uses mathematical and statistical techniques to link input variables (factors) to the response variables [36]. RSM has been effectively used to optimize parameters in research, engineering, and technology [5,21,37–40].

Therefore, RSM was used in this study is to optimize three process variables of the polyesterification process: (1) reaction time, (2) ratio of EG to UCOCI methyl ester, and (3) sodium methoxide catalyst concentration. The process variables were optimized to maximize the UCOCI biolubricant yield and minimize the energy consumption of the biolubricant production process. In addition, the physicochemical properties of the biolubricant were compared with those of the SAE 15W-40 commercial synthetic lubricant as well as those specified in other lubricant standards. Subsequently, the UCOCI biolubricant and its blends were tested to determine their tribological characteristics to assess the viability of the UCOCI biolubricant as an alternative lubricant.

2. Materials and methods

2.1. Materials

The feedstocks used in this study were UCO obtained from a city farm and CIO from Central Java, Indonesia. The reagents used in this study were methanol (Merck, purity $\geq$ 99.9 %), sulphuric acid (Merck, purity $>$ 98.9 %), orthophosphate (Merck, purity $\geq$ 85 %), potassium hydroxide (KOH) pellets (Merck, purity $\geq$ 99 %), sodium methoxide (CH_3ONa) pellets (Pallav, purity $\geq$ 98 %), phenolphthalein solution (1 % in ethanol), and Shell SAE 15W-40 synthetic lubricant. For the tribological tests, the materials used were a cleaning solvent (acetone), a rinser (n-heptane), and a chromium alloy steel test ball with a diameter of 12.7 mm (0.5 in.), Grade 25 EP (extra polished) and Rockwell C hardness of 64–66.

2.2. Experimental set-up

The infrared irradiation-assisted reactor used for biolubricant production consisted of 500 mL of transparent borosilicate glass (without a jacket and with a thickness of 5 mm) equipped with infrared light (input speed: 100 W, voltage: 220 V, frequency: 50 Hz) to produce infrared energy in the range of 0.001–1.7 eV Infrared radiation was used to accelerate the process of esterification and transesterification. A 100-W infrared light was placed inside the 500-mL glass reactor connected to a magnetic mixer. The magnetic mixer was used to ensure homogeneous mixing of the reaction mixture in the borosilicate reactor. Fig. 1 shows the schematic of the experimental set-up used for biolubricant synthesis assisted by infrared irradiation. This experimental set-up was used for acid-catalysed esterification and alkaline-catalysed transesterification.

2.3. Pre-treatment and selection of oil blend for biolubricant production

In the first stage, the collected UCO was filtered using a filter paper to remove food residues from the oil. Next, the UCO was heated to a temperature of 100 °C for 60 min to minimize the water content of the oil. Pre-treatment was carried out due to the high acidity of the UCO and CIO. This procedure facilitates the elimination of particles or contaminants present in the oil during extraction or due to atmospheric exposure. Contaminants may present a challenge during the esterification and transesterification processes, which can reduce the quality of the biolubricant. Therefore, it is imperative to perform the pre-treatment at high temperatures. First, 1 kg of CIO was measured and poured into a beaker placed on top of the heating element. Subsequently, the CIO was heated at 100 °C, the CIO was stirred for 1 h at a stirring speed of 500 rpm, the CIO was left to cool for 15 min, and subsequently, the CIO was filtered to eliminate solid impurities. [41]. After pre-treatment of the UCO and CIO, the UCO and CIO were mixed at a volume ratio of 70:30, producing the UCOCI oil blend. The oxidation stability, acid value, and free fatty acid content of pure UCO (UCO100), pure CIO (CIO100), and their blends are summarised in Table 1. It can be seen that the oxidation stability, acid value, and free fatty acid content increased with an

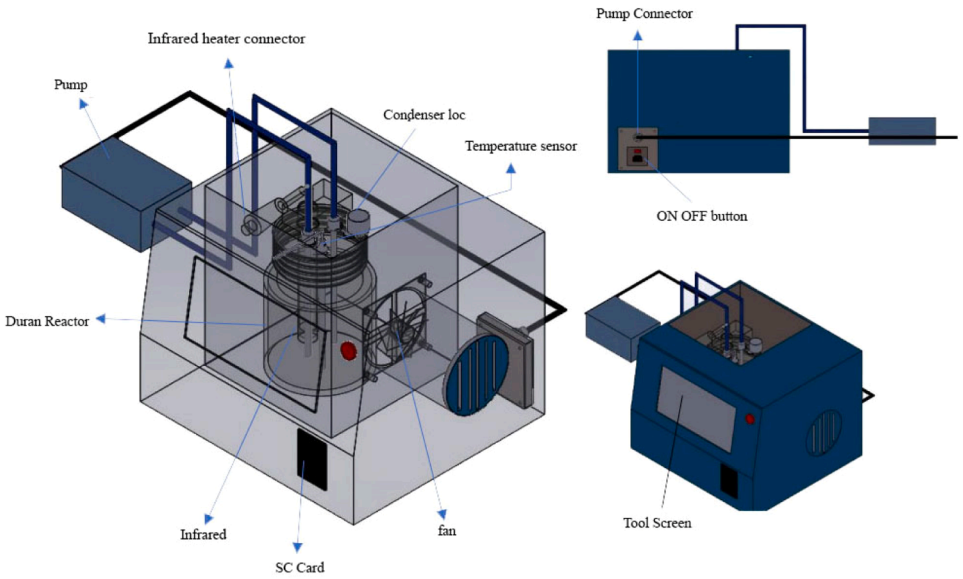

Fig. 1. Infrared irradiation-assisted reactor for biolubricant synthesis.

Table 1
Properties of pure UCO, pure CIO, and their blends.

Property	Units	Raw oil blend					
		UCO100	CIO100	UC90CI10	UC80CI20	UC70CI30	UC60CI40
Oxidation stability	min	77.6	588.34	98.6	128.1	207.27	258.23
Acid value	mg KOH/g	2.21	62.23	7.98	13.95	18.94	28.72
Free fatty acid content	%	1.17	29.72	3.91	6.982	9.83	13.64

increase in the percentage of CIO in the blend.

It is evident from Table 1 that the oxidation stabilities of the UC90CI10 and UC80CI20 blends were relatively low, and thus, these oil blends were not explored further. In contrast, the oxidation stabilities were higher for the UC70CI30 and UC60CI40 blends, and therefore, these blends appeared to be promising for biolubricant production. However, the acid values for the UC70CI30 and UC60CI40 blends were high, with a value of 18.94 and 28.72 mg KOH/g respectively. The UC60CI40 blend required a double esterification process, which would increase the cost of biolubricant production. Hence, the UC70CI30 blend was selected for biolubricant production in this study by esterification and double transesterification using infrared technology.

2.4. Biolubricant production

2.4.1. Degumming process

Degumming process was conducted on the crude oils to improve their oxidation stability. Crude oils typically contain various quantities of phosphatides (gums), which must be eliminated from the oils before the transesterification process. The process of separating gums consisting of phosphatides, protein residues, carbohydrates, water, and resins is called degumming. In this stage, the UCOCI oil blend was inserted into a double jacketed reactor added with 5 % (v/v) of 20 % (v/v) phosphoric acid (H_3PO_4) heated at a temperature of 60 °C, and stirred at a stirring speed of 800 rpm for 30 min [21]. Following this, filtration was carried out on the UCOCI oil blend using a separatory funnel for 2–4 h, resulting in the accumulation of phosphatides at the base of the funnel. The resultant UCOCI oil blend was then washed with warm distilled water at 45–50 °C 2–3 times. The degumming process was similar to the procedure performed by Milano et al. [21].

2.4.2. Acid-catalysed esterification

It is necessary to minimize the free fatty acids of the crude oil blend because a high acid value can result in significant saponification. The high FFA content of the UCOCI oil blend was reduced by esterification with methanol using sulphuric acid as a catalyst [16]. The transesterification reaction cannot be catalysed by a homogeneous alkaline catalyst when the FFA content is greater than 3 % [16]. To address this problem, acid-catalysed esterification was carried out on the UCOCI oil blend.

In this process, 500 mL of UCOCI oil blend was mixed with a solution containing 1 % (v/v) of sulphuric acid (H_2SO_4) and a 20 % (v/v) of methanol. Next, the mixture was moved into infrared irradiation-assisted reactor. The UCOCI oil blend was stirred at a temperature of 60 °C and stirring speed of 500 rpm for 60 min. To facilitate the separation of impurities from the UCOCI oil blend, the UCOCI oil blend was poured into a separatory funnel once the reaction was complete and left for 2 h The esterified UCOCI oil blend was then collected and placed in a rotary evaporator under vacuum and heated at 80 °C for 30 min. The main purpose of this was to get rid of any remnants of methanol in the esterified UCOCI oil blend. The details of the acid-catalysed esterification are similar to those of other studies [11,16,21,29].

2.4.3. Alkaline-catalysed transesterification

In this stage, alkaline-catalysed transesterification was carried out on the esterified UCOCI oil blend, which already had a low acidity. Excess methanol (99.9 %) was required to drive the transesterification reaction forwards, producing UCOCI methyl ester and glycerol [42]. The esterified UCOCI oil blend was mixed with 1 % (w/w) of KOH catalyst and 25 % (v/v) of methanol (CH_3OH). The transesterification was conducted at a temperature of 60 °C and stirring speed of 500 rpm for 60 min. The alkaline-catalysed transesterification was similar to those of other studies [11,16,21,29,42].

After the transesterification process was complete, sedimentation was carried out over a certain period to separate the glycerol from the UCOCI methyl ester. The upper layer consisted of the UCOCI methyl ester, while the lower layer was a mixture of glycerol and other detergents removed from the splinter. The UCOCI methyl ester was washed with warm water several times and then poured into a vacuum evaporator set at a temperature of 70 °C to remove moisture and excess methanol. Lastly, the UCOCI methyl ester was filtered. The UCOCI methyl ester is shown in Fig. 2.

2.4.4. Polyesterification

In this stage, polyesterification was carried out on the UCOCI methyl ester, which had a low acid value. Polyesterification is also called second-stage transesterification. Polyesterification is the process of synthesizing the UCOCI methyl ester with EG and sodium methoxide (CH_3ONa) catalyst [42]. The EG and sodium methoxide catalyst were mixed with 400 mL of UCOCI methyl ester. The following polyesterification process variables were varied according to the Box–Behnken experimental design: (1) reaction time: 30, 75, and 120 min, (2) ratio of EG to UCOCI methyl ester: 20, 30, and 40 % (v/v), and (3) sodium methoxide concentration: 0.5, 1, and 1.5 % (w/w). The temperature and stirring speed of the infrared irradiation-assisted reactor were set at 125 °C and 300 rpm, respectively. After the polyesterification process was complete, separation was carried out over a certain period to separate glycerol from the UCOCI biolubricant. After the removal of by-products and sodium methoxide catalyst from the lower layer, the UCOCI biolubricant was washed with distilled water at 40 °C to remove any remaining contaminants. The UCOCI biolubricant was subsequently evaporated using a rotary evaporator under vacuum at 70 °C, followed by filtration using Whatman 541 filter paper. The details of the biolubricant production are described in previous studies [26,38,39,42,43]. The biolubricant yield was determined using Eq. (1):

$$\text{Biolubricant yield}\,(\%(\text{w}/\text{w})) = \frac{\text{Weight of UCOCI biolubricant obtained}\ (\text{g})}{\text{Weight of UCOCI methyl ester used}} \times 100 \quad (1)$$

2.4.5. Optimization of the polyesterification process variables by RSM

RSM based on Box–Behnken experimental design was adopted in this study maximize the UCOCI biolubricant yield. Design-Expert® version 13.0.1.0 software was employed to optimize the polyesterification process variables, namely, (1) reaction time (x_1), (2) ratio of EG to UCOCI methyl ester (x_2), and (3) sodium methoxide catalyst concentration (x_3). The UCOCI biolubricant yield served as the dependent variable (response variable), whereas the polyesterification process variables served as the independent variables (factors). The UCOCI biolubricant yields obtained for different process variables were compared. Each independent variable was coded as −1, 0, and +1, as presented in Table 2.

Fig. 2. UCOCI methyl ester.

Table 2
Selected polyesterification process variables and their coded levels according to the Box–Behnken experimental design.

Symbol	Independent variable	Unit	Coded levels		
			−1	0	1
x_1	Reaction time	min	30	75	120
x_2	Ethylene glycol concentration	% (v/v)	20	30	40
x_3	Sodium methoxide catalyst concentration	% (w/w)	0.5	1	1.5

Based on Table 2, 17 experimental runs were necessary to examine the interaction effects of the independent variables. The Box–Behnken experimental design encompassed all combinations of independent variables at every level in a perfectly randomized sequence [44]. Analysis of variance (ANOVA) was then carried out to determine the statistical significance of the independent variables and their interactions.

2.5. Characterzsation of the UCOCI biolubricant

Evaluation of the physiochemical properties of SAE 15W-40 lubricant and UCOCI biolubricant

The density, kinematic viscosities at 40 and 100 °C, and viscosity index (VI) of the UCOCI biolubricant and SAE 15W-40 commercial synthetic lubricant were measured using a viscometer in accordance with the ASTM D7042 standard. High-viscosity lubricants are deemed to be suitable for extreme environments, such as hydraulic and automotive applications. Conversely, low-viscosity lubricants are recommended for small equipment such as pumps and chainsaws. The VI indicates the extent to which the viscosity of the lubricant is altered in response to changes in temperature. For industrial applications and extreme environments, a high VI is necessary. The acid value, flash point, and oxidation stability of the lubricants were evaluated according to the ASTM D664 and ASTM D93 standards.

2.5.1. Tribological characteristics of the UCOCI biolubricant and its blends

The tribological characteristics (coefficient of friction and wear scar diameter) of the UCOCI biolubricant and its blends were measured using a four-ball tribotester, as shown in Fig. 3. Five UCOCI biolubricant blends were produced, namely, Biol10 Biol20, Biol30, Biol40, and Biol50, containing 10, 20, 30, 40, and 50 % of SAE 15W-40 synthetic lubricant, respectively. Prior to the tribotests, the four new balls, ball pots, ball locking rings, bearing plates, and collets were thoroughly cleaned using n-heptane and then left to dry. Following this, one ball was pressed into the ball collet using the ball inserter or ejector mounted on the test rig base plate and the collet was inserted into the spindle. The ball pot assembly was placed on top of the base plate slot. The locking ring was lifted, the three clean balls were inserted into the cavity, the locking ring was lowered to hold the ball in position, and the locking nut was locked using the specified torque value.

According to the ASTM standard, the recommended value of torque should be 68 Nm or 50 ft-lbs. The lubricant sample was filled above 3 mm of the ball surface. The loading arm was lifted, the loading lever was held, and the ball pot assembly was placed on top of the anti-friction disc, ensuring that the anti-friction disc was properly aligned over the

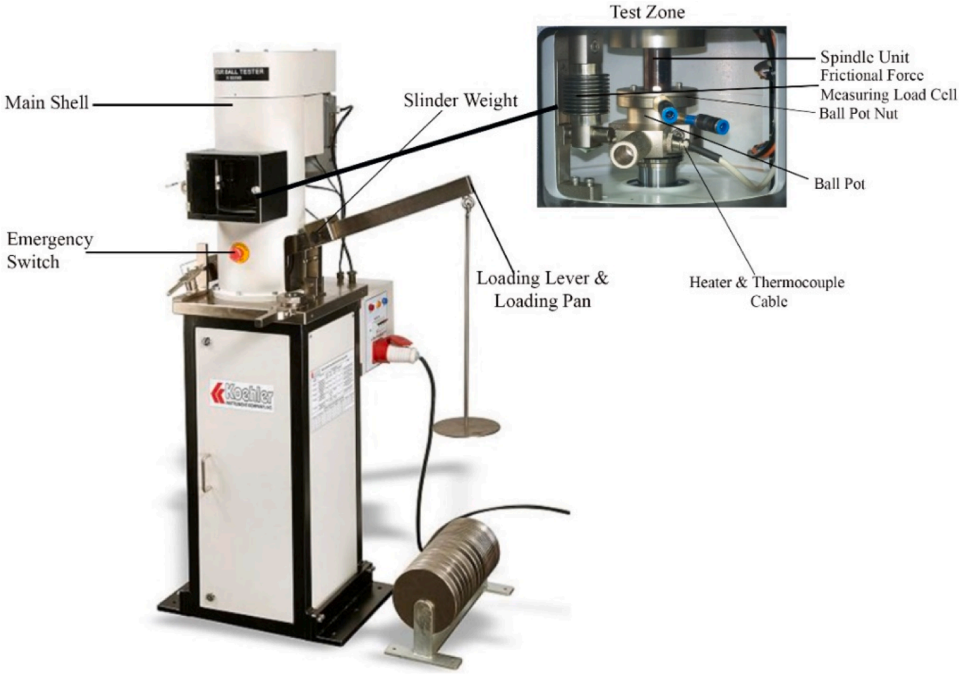

Fig. 3. Four-ball tribotester used to evaluate the tribological characteristics of the UCOCI biolubricant and its blends.

thrust pad. A thin layer of lubricant sample was applied over the anti-friction disc and the loading lever assembly was lowered. By removing the loading arm holder and connecting the heating cable to the ball pot, it is important to ensure that the loading lever arm is lowered slowly without any impact on the ball surface. The pan weight loading arm die was set according to the value recommended in the ASTM standard d4172. After performing the load release test, the loading arm was lifted and locked, the acrylic door was opened, and the anti-friction disc was removed. After welding was done, the ball pot remained attached to the collet. The collector extractor was inserted into the spindle slot. The ball pan was held, and the extractor was pressed down to release the heating cable and collet, ensuring that the ball pot assembly was kept in the ball pot slot on the base plate. The assembly was allowed to cool, the collet was pulled using a pair of pliers, the lock nut was unscrewed, the lubricant sample was removed, and the ball pot was cleaned for further testing. If welding had not yet occurred, the ball pot assembly was removed after disconnecting the heating cable, stored in the ball pot slot in the base plate, and left to cool.

Four-ball wear tests were carried out on the lubricant sample according to the ASTM D4172–94 standard with a test duration of 3600 s at a temperature of 75 °C, spindle speed of 1200 rpm, and load of 40 kg. The four-ball wear test procedure was also adopted in other studies [34,45,46]. The coefficient of friction was determined by multiplying the mean friction torque by the spring constant. Consequently, the frictional torque on the lower ball can be determined from the following equation:

$$T = \frac{\mu \times 3W \times r}{\sqrt{6}} \rightarrow \mu = \frac{T\sqrt{6}}{3W \times r} \quad (2)$$

where μ is the coefficient of friction, r is the distance from the centre of the contact surface on the lower balls to the axis of rotation (which is 3.67 mm), T is the frictional torque (kg·mm), and W is the applied load (kg). The wear scar diameter was measured and analysed using an image acquisition system.

Table 3
Box–Behnken experimental design of the infrared irradiation-assisted sodium methoxide-catalysed polyesterification process.

Experimental run	A: Reaction time (min)	B: Ratio of EG to UCOCI methyl ester (% (v/v))	C: Sodium methoxide catalyst concentration (% (w/w))	Experimental UCOCI biolubricant yield (%)	Predicted UCOCI biolubricant yield (%)
15	120	20	1	83.8906	83.83318
4	30	20	1	84.7191	84.66956
3	75	20	1.5	86.7580	87.14138
16	30	30	0.5	79.5290	79.85026
14	120	30	0.5	81.7130	82.04917
17	75	30	1	94.0208	94.30179
6	75	30	1	94.1900	94.30179
8	75	30	1	94.1907	94.30179
11	75	30	1	94.2808	94.30179
9	75	30	1	94.8080	94.30179
13	30	30	1.5	78.8830	78.55517
12	120	30	1.5	78.9618	78.64889
10	75	40	0.5	87.6670	87.29151
5	30	40	1	80.4233	80.48930
7	120	40	1	83.5598	83.61832
2	75	40	1.5	88.3147	88.58827

3. Results and discussion

3.1. Optimization of the polyesterification process variables by RSM

As mentioned in Section 2, RSM based on the Box–Behnken design was used to optimize the infrared irradiation-assisted sodium methoxide-catalysed polyesterification process variables to maximize the UCOCI biolubricant yield. The experimental design consisted of 17 trials, each with three process variables (reaction time, ratio of EG to UCOCI methyl ester, and sodium methoxide catalyst concentration) and three levels. The UCOCI biolubricant yields obtained from the experiments are summarised in Table 3 and were compared with the predicted UCOCI biolubricant yields.

Based on the results shown in Table 3, the UCOCI biolubricant yield varied from 78.883 % to 94.808 %. The UCOCI biolubricant yield (Y) can be predicted from the reaction time (A), ratio of EG to UCOCI methyl ester (B), and sodium methoxide catalyst concentration (C) using the following quadratic equation:

$$Y = 94.24 + 0.5877A - 1.17B - 0.8731C + 0.9787AB - 0.5027AC + 2.4\ BC - 10.67A^2 - 0.4544B^2 - 3.87C^2 \quad (3)$$

Eq. (3) delineates the quadratic response surface model used to predict the UCOCI biolubricant yield based on the parameters of the polyesterification process (uncoded independent variables). The UCOCI biolubricant yields predicted using this model are tabulated in Table 3. It is apparent that the UCOCI biolubricant yields obtained from experiments conformed well with those predicted by the quadratic response surface model.

ANOVA was used to assess the validity of the quadratic response surface model, and the results are presented in Table 4. It can be seen that the quadratic response surface model had a large F-value (375.27) and low p-value ($p < 0.0001$) at 99 % confidence interval, indicating that model was statistically significant. Based on the results, factors A, B, C, AB, AC, BC, A^2, B^2, and C^2 were significant model terms since the p-values were <0.05. If the p-value of the model term is greater than 0.05, the model term is not statistically significant.

Fig. 4 shows the normal probability plot of the externally studentized residuals and it is evident that the residuals were well-behaved, where the residuals were close to the diagonal line, suggesting that the model is valid. Fig. 5 shows the comparison between the predicted and experimental UCOCI biodiesel yields and it can be observed that the values showed good agreement. In addition, the coefficient of determination (R^2) of the model exceeded 90 %, indicating the high significance of each model term [47]. The R^2 value is a statistical measure that shows how well the predicted values of the model are in line with the actual values observed [47]. It can be seen from Table 4 that the R^2 value of the model was 0.9979, signifying that 99.79 % of the variability in the response variable (UCOCI biolubricant yield) is explained by the variability in the independent variables (reaction time, ratio of EG to UCOCI methyl ester, and sodium methoxide catalyst concentration). The high R^2 value indicates that the model effectively explains most of the variability in the UCOCI biolubricant yield. An R^2 value close to 1 indicates that the values predicted by the model are close to those obtained from experiments [48] The high R^2 value indicates the reliability of the RSM adopted in this study and shows that the model is very consistent with the data and can be trusted to predict the results under optimal conditions [5]. Silitonga et al. [16] validated the response surface model and produced *Reutealis trisperma* methyl ester (RTME) by intensification process assisted by infrared radiation using process variables optimized by RSM. The experiment was performed three times and the average RTME yield was determined to be 97.78 %, which was close to the predicted RTME yield of 98.39 %.The coefficient of variation (CV) is the standard deviation divided by the mean. The higher the CV, the higher the dispersion around the mean, and therefore, a low CV indicates that the experiment has high dependability and precision [40]. In this study, the CV was 0.4815 %, indicating that the experiment has substantial reliability and precision. The adequate precision (signal-to-noise ratio)

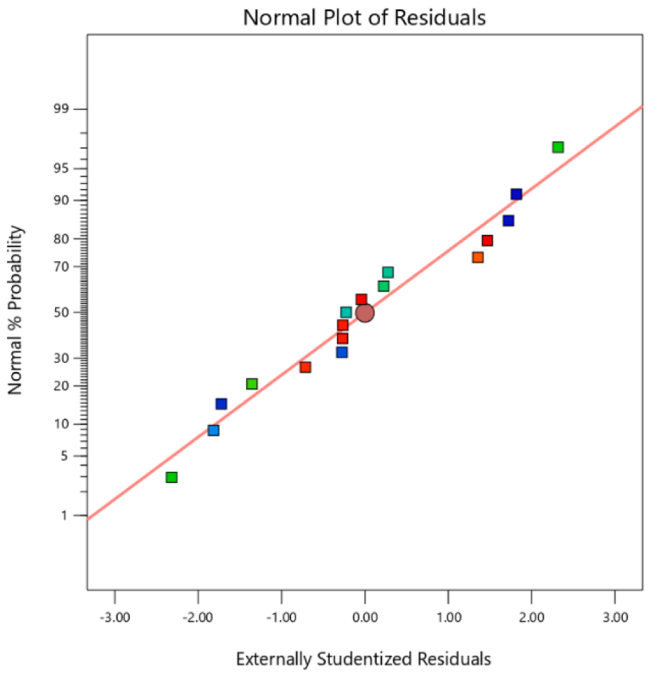

Fig. 4. Normal probability plot of externally studentized residuals.

Table 4
ANOVA results for the quadratic response surface model used to predict the UCOCI biolubricant yield.

Source	Sum of squares	Degree of freedom	Mean square	*F*-value	*p*-value	
Model	592.84	9	65.87	375.27	< 0.0001	Significant
A-Reaction time	2.61	1	2.61	14.88	0.0062	
B-Ratio of EG to UCOCI methyl ester	9.68	1	9.68	55.17	0.0001	
C-Sodium methoxide catalyst concentration	11.02	1	11.02	62.8	< 0.0001	
AB	3.93	1	3.93	22.39	0.0021	
AC	1.11	1	1.11	6.31	0.0403	
BC	13.28	1	13.28	75.67	< 0.0001	
A^2	438.62	1	438.62	2498.83	< 0.0001	
B^2	3.75	1	3.75	21.35	0.0024	
C^2	78.58	1	78.58	447.65	< 0.0001	
Residual	1.23	7	0.1755			
Lack of fit	0.8683	3	0.2894	3.21	0.1446	No significant
Pure error	0.3604	4	0.0901			
Cor total	594.07	16				

CV = 0.4815 %; R^2 = 0.9979; R^2Adj = 0.9953; Predicted R^2 = 0.9757; Adeq Precision = 49.004.

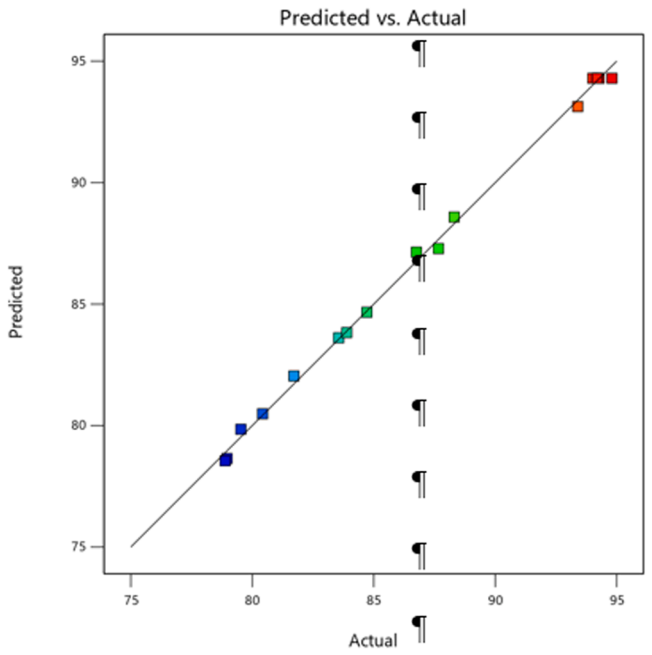

Fig. 5. Comparison between the experimental and predicted UCOCI biolubricant yields.

was also assessed in this study, and a ratio over 4 is preferred. It can be seen from Table 4 that the adequate precision was 49.00, indicating adequate model discrimination. The residual is the discrepancy between the observed value and estimated value. Each observation in the dataset has a residual. The estimated residuals follow a Gaussian distribution if the experimental error is random. Hence, it is crucial to evaluate the adequacy of the quadratic response surface model to determine if the residuals conform to a normal distribution.

3.2. Optimization of the infrared irradiation-assisted polyesterification process using RSM

As discussed earlier, RSM was used to optimize the process variables of the infrared irradiation-assisted sodium methoxide-catalysed polyesterification process. The optimum reaction time, ratio of EG to UCOCI methyl ester, and sodium methoxide catalyst concentration were 77.438 min, 23.448 % (v/v), and 1.02 % (w/w), respectively. Using the quadratic response surface model (Eq. (1)), the predicted UCOCI biolubricant yield was 95.150 %, obtained using the optimum process variables.

It can be deduced that the use of infrared radiation facilitates the conversion of free fatty acids into methyl ester. The infrared energy (photons with energy levels of 0.001–1.7 eV) corresponds to the range of energy that separates the molecular vibration's quantum state. As a result, the infrared radiation can penetrate deeper into the reaction mass compared with visible radiation. Furthermore, more intense infrared radiation is absorbed compared with conventional microwaves and thermal energy [16,43]. Numerous studies have reported that the transesterification of vegetable oil triester with TMP, NPG, EG, and PET as polyols for average biolubricant synthesis using conventional reactors requires a reaction time of 4–6 h [5,10,25,31–34]. Infrared radiation interacts with the molecules of the reaction mass, putting them into vibration mode and causing severe molecular collisions. In contrast with conventional reactors, infrared irradiation-reactors can improve the direct transfer of heat energy to the reactant molecules, thereby substantially augmenting the activation of their active species [49]. Silitonga et al. [16] obtained an average RTME yield of 97.78 %, indicating that infrared irradiation-assisted transesterification has many advantages, such as lower energy consumption due to the deeper penetration of the infrared radiation into the reaction mass, which can increase mass transfer between non-mixable reactants, thereby improving the biodiesel quality. Therefore, it can be deduced that the infrared irradiation-assisted sodium methoxide-catalysed polyesterification process is efficient and suitable to produce biolubricants, and the biolubricant yield can be boosted by using the optimum process variables.

3.3. Effects of polyesterification process variables on the UCOCI biolubricant yield

Three-dimensional response surface plots were constructed to analyse the effects of the process variables (reaction time, ratio of EG to UCOCI methyl ester, and sodium methoxide catalyst concentration) on the UCOCI biolubricant yield. The plots help identify the process variables that have a more substantial effect on the UCOCI biolubricant yield.

3.3.1. Effects of ratio of EG to UCOCI methyl ester and reaction time

Fig. 6 shows the effects of the ratio of EG to UCOCI methyl ester (20–40 % (v/v)) and reaction time (30–120 min) on the UCOCI biolubricant yield. The optimum ratio of EG to UCOCI methyl ester was within a range of 20–40 % (v/v). The reversible nature of the transesterification reaction [36] and the diffusion of the reaction mixture [42] results in a reduced conversion of free fatty acids into triesters as the volumetric ratio of EG increases [24]. The disparity in the concentrations of UCOCI methyl ester and EG in contact generates a driving force that accelerates the mass transfer rate of the UCOCI biolubricant. This is also confirmed by Ifeanyi-Nze et al. [42], who found that the ratio of EG to fatty acid methyl ester had a direct impact on the triester polyols that produced the biolubricant, where an increase in the ratio of EG to fatty acid methyl ester increased the conversion of free fatty acids into triesters, increased the molar ratio of the reactants above the stoichiometric value, and improved the output of the biolubricant. The ratio of EG to fatty acid methyl ester plays a vital role in the transesterification process to produce biolubricant [50]. Fig. 6 shows that the optimum reaction time that maximized the UCOCI biolubricant yield was 73 min. The red region of the response surface plot indicates the optimum UCOCI biolubricant yield.

3.3.2. Effects of sodium methoxide catalyst concentration and reaction time

Fig. 7 shows the effects of reaction time (30–120 min) and sodium

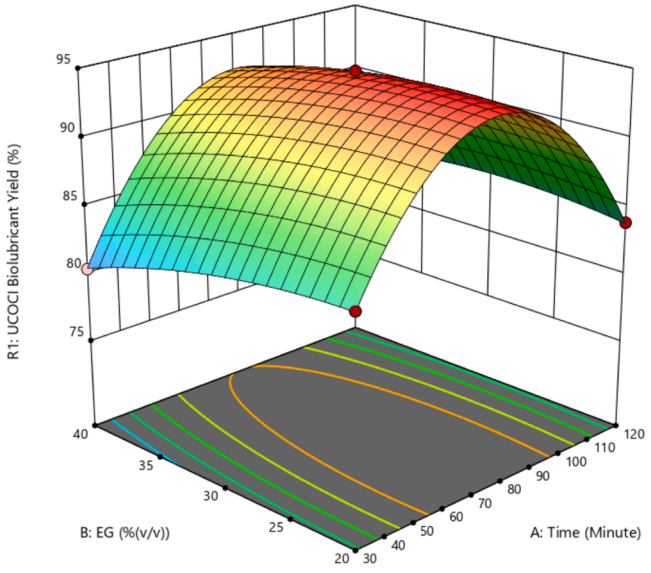

Fig. 6. Response surface plot showing the effects of the ratio of EG to UCOCI methyl ester and reaction time on the UCOCI biolubricant yield.

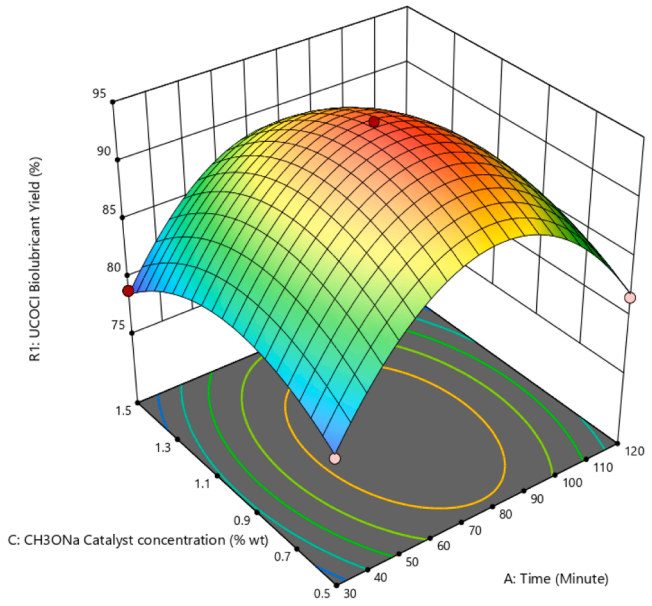

Fig. 7. Response surface plot showing the effects of sodium methoxide catalyst concentration and reaction time on the UCOCI biolubricant yield.

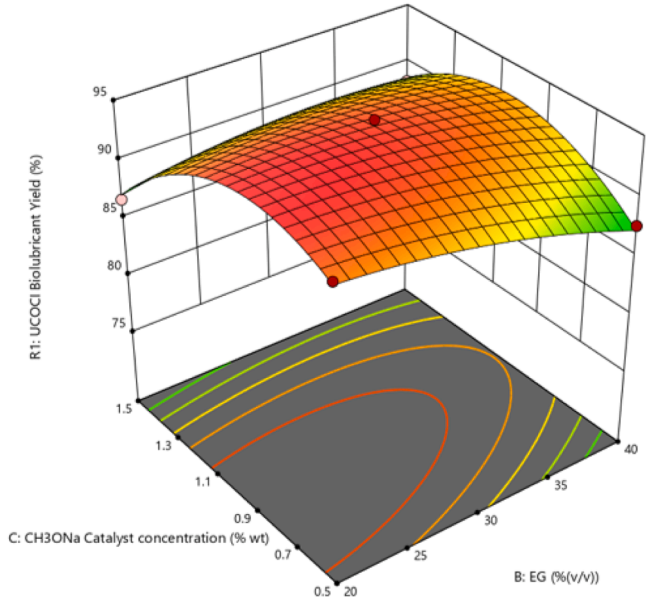

Fig. 8. Response surface plot showing the effects of sodium methoxide catalyst concentration and ratio of EG to UCOCI methyl ester on the UCOCI biolubricant yield.

methoxide catalyst concentration (0.5–1.5 % (w/w)) on the UCOCI biolubricant yield. The UCOCI biolubricant yield increased as the reaction time increased from 60 min to 90 min, followed by a gradual decrease thereafter. This indicates that the reaction time plays a pivotal role in accelerating or decelerating the polyesterification reaction. Infrared irradiation is perceived to enhance the thermal energy of reactants during the transesterification reaction with alkali catalyst that facilitate the synthesis of methyl ester [16,51].

3.3.3. *Effects of sodium methoxide catalyst concentration and ratio of EG to UCOCI methyl ester*

Fig. 8 shows the effects of sodium methoxide catalyst concentration (0.5–1.5 % (w/w)) and ratio of EG to UCOCI methyl ester (20–40 % (v/v)) on the UCOCI biolubricant yield. The UCOCI biolubricant yield only exhibited a marginal increase as the sodium methoxide catalyst concentration increased from 0.75 % (w/w) to 1.2 % (w/w), suggesting that the concentration of sodium methoxide catalyst can enhance the UCOCI biolubricant yield only to a limited extent. The UCOCI biolubricant yield decreased at sodium methoxide catalyst concentrations of >1.2 % (w/w) due to saponification.

The results were consistent with those of Silitonga et al. [16], who obtained an optimum RTME yield at a KOH catalyst concentration of 1 % (w/w). They performed transesterification without infrared irradiation and used an alkali catalyst to produce biodiesel. Fig. 8 also shows that the ratio of EG to UCOCI methyl ester had a pronounced effect on the UCOCI biolubricant yield, exceeding the effect of the sodium methoxide catalyst concentration. The UCOCI biolubricant yield reached its maximum when the ratio of EG to UCOCI methyl ester was 30 % (v/v).

3.4. *Physicochemical properties of the crude UCO and CIO, UCOCI methyl ester, and UCOCI biolubricant*

The physicochemical properties of the UCOCI methyl ester (produced from UC70CI30 oil blend), SAE 15W-40 lubricant, and UCOCI biolubricant were determined and compared with those specified in ISO VG 32, ISO VG 46, ISO VG 68, and ISO VG 100 lubricant standards, as shown in Table 5. The kinematic viscosity at 40 °C and density at 15 °C of the UCOCI methyl ester were 5.717 cSt and 860.83 kg/m^3, respectively Once the UCOCI methyl ester was converted into UCOCI biolubricant by polyesterification, the kinematic viscosities at 40 and 100 °C of the UCOCI biolubricant were 83.46 and 13.2 cSt, respectively. However, the kinematic viscosities of the SAE 15W-40 lubricant were higher than those of the UCOCI biolubricant, which was similar to the results of Gul et al. (2021), who found that the kinematic viscosity of the SAE 15W-40 lubricant was higher than that of the cotton seed biolubricant.

The kinematic viscosity of the lubricant is the most critical attribute since deviations from the desired values specified in the lubricant standards may lead to system malfunction. A stable viscosity over a wide range of temperatures is preferred when choosing a lubricant [52]. One numerical indicator of the influence of temperature on lubricant viscosity is the viscosity index (VI). A low VI indicates that the viscosity is temperature-dependent, resulting in thinner oil at elevated temperatures and significantly thicker oil at lower temperatures [42]. In contrast, a high VI indicates that the viscosity of the lubricant only slightly changes over a wide temperature range. A higher VI suggests better lubricant quality [34]. The VI of the UCOCI biolubricant (Biol100) was determined to be 216.32 (Table 5). The addition of EG and sodium methoxide catalyst into the UCOCI methyl ester resulted in the highest kinematic viscosity and VI, with values that were nearly equal to those for the SAE 15W-40 lubricant (99.2 cSt and 136.14) and ISO VG 100 standard.

The flash point is defined as the minimum temperature at which the lubricant evaporates and forms a flammable mixture with air. The flash point is a measure of the risk of fire hazards of the lubricant [46]. It can be observed from Table 5 that the flash point of the UCOCI biolubricant was 243.3 °C, which was higher than that of the SAE 15W-40 lubricant (230 °C), and close to the flash point specified in the ISO VG 100 standard. The average commercial lubricant has a flash point greater than 200 °C [10,53–55]. The kinematic viscosity and flash point of the lubricant have a significant effect on the flow characteristics and atomization of the lubricant. The viscosity and flash point of biolubricants can be affected by the presence of impurities (such as free glycerol and glycerides) and temperature [46].

Oxidation stability is one of the important properties of a lubricant. Oxidation stability predicts the lifespan of the lubricant, especially in high-temperature conditions [11]. It can be seen from Table 5 that the SAE 15W-40 lubricant had higher oxidation stability (1703.2 min) than the UCOCI biolubricant (1642.67 min). The oxidation stability of

Table 5
Comparison of the physicochemical properties of crude UCO and CIO, UCOCI methyl ester, and UCOCI biolubricant against those of the SAE 15W-40 commercial synthetic lubricant and lubricant standards.

Property	Unit	UCO	CIO	UC70CI30 oil blend	UCOCI methyl ester	UCOCI biolubricant (Biol100)	Lubricant standards				
							SAE 15W-40	ISO VG 32	ISO VG 46	ISO VG 68	ISO VG 100
Kinematic viscosity at 40 °C	cSt	47.9	63.38	51.27	5.717	83.46	99.2	> 28.8	> 41.1	> 61.4	> 90
Kinematic viscosity at 100 °C	cSt	—	—	—	—	13.2	13.7	> 4.1	> 4.1	> 4.1	> 4.1
Density at 15 °C	kg/m^3	901.68	923.4	909.2	860.83	—	—	—	—	—	—
Viscosity index	—	—	—	—	—	216.32	136.14	> 90	> 90	> 198	> 216
Flash point	°C	—	—	—	165.3	243.3	230	204	220	226	246
Oxidation stability at 110 °C	min	77.6	588.34	207.27	1043.4	1642.67	1703.2	—	—	—	1670.26
Acid value	mg KOH/g	2.21	62.23	18.94	0.46	0.447	0.73	—	—	—	—

Fig. 9. UCOCI biolubricant.

biomass can lead to polymerization and higher viscosity [56]. Epoxidation, solid formation, and hydrogenation can all increase the oxidation stability of non-edible oils that are chemically modified through esterification and transesterification reactions [23,25]. The UCOCI biolubricant is shown in Fig. 9.

3.5. Tribological characteristics of the UCOCI biolubricant

3.5.1. Coefficient of friction

The UCOCI biolubricant was blended with the SAE 15W-40 commercial synthetic lubricant in various proportions (Biol10 (10 % synthetic lubricant), Biol20 (20 % synthetic lubricant), Biol30 (30 % synthetic lubricant), Biol40 (40 % synthetic lubricant), and Biol50 (50 % synthetic lubricant)) to assess their tribological characteristics. A four-ball tribotester was used for this purpose, in accordance with the ASTM D4172–94 standard. All of the lubricants possess the fundamental ability to establish and sustain a stable lubricating layer in the metal contact area. This is indeed expected since biolubricant has superior lubrication performance owing to its ester functionality [46]. Fig. 10 shows the variation of the coefficient of friction for the lubricant samples subjected to a load of 400 N at a temperature of 75 °C for 3600 s (60 min).

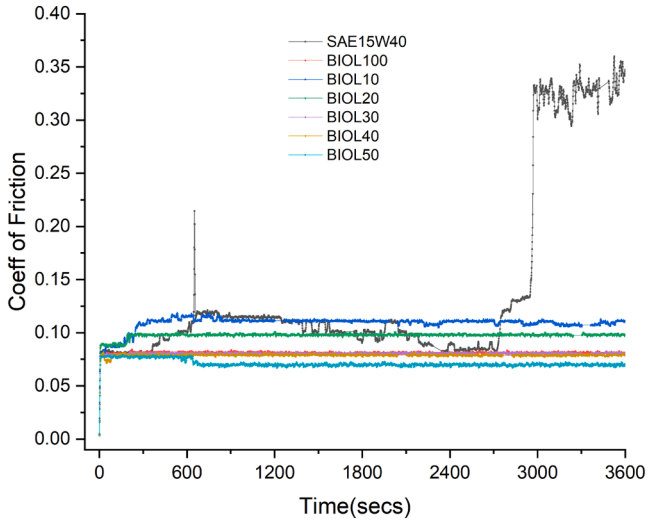

Fig. 10. Variations of the coefficient of friction of the lubricant samples and SAE 15W-40 commercial synthetic lubricant with respect to time.

At the start of each experiment, there was a substantial reduction in the coefficient of friction for all of the lubricant samples tested in this study. The coefficient of friction for each lubricant sample achieved steady-state condition after 30 s from the start of the experiment. It is evident that the lubricant samples had lower coefficients of friction compared with the SAE 15W-40 lubricant, which is likely due to the high unsaturated fatty acids and lower saturated fatty acids of the UCOCI biolubricant. The UCOCI biolubricant (Biol100) exhibited the lowest coefficient of friction compared with other lubricants. The SAE 15W-40 lubricant exhibited the highest coefficient of friction after 40 min of experimentation. Fig. 10 and Table 6 show the average coefficients of friction of the UCOCI biolubricant and its blends and the SAE 15W-40 commercial synthetic lubricant.

It can be seen from Table 6 that the average coefficient of friction of the UCOCI biolubricant (Biol100) was 0.0811, which was significantly lower than that of the SAE 15W-40 commercial synthetic lubricant. The Biol10, Biol20, Biol30, Biol40, and Biol50 lubricants also exhibited outstanding lubrication performance under the same experimental settings, where the average coefficients of friction were 0.1091, 0.0975, 0.0803, 0.0788, and 0.071, respectively. Kalam et al. [46] also obtained similar results, where the coefficient of friction of the biolubricant produced from olive oil (0.076) was lower than that of SAE 15W-40 lubricant (0.092) and reached a steady-state value after 30 s from the start of the experiment. The SAE 15W-40 lubricant resulted in higher friction over extended periods. Abdollah, Amiruddin, and Jamallulil (2020) compared the coefficient of friction of the SAE 15W-40 lubricant (0.115) with those of palm oil (0.080), palm oil blended with 0.1 % of hexagonal boron nitride nanoparticles (0.079), and palm oil blended with 0.5 % of hexagonal boron nitride nanoparticles (0.110). Based on these findings, it can be deduced that the coefficients of friction of biolubricants produced from edible and non-edible oils are lower than that of SAE 15W-40 commercial synthetic lubricant (0.110). The coefficient of friction of biolubricant produced from waste cooking oil was 0.06 (Joshi et al. [6]) while the coefficients of friction for biolubricants produced from rice bran oil and TMP cotton tricyst were 0.073 (Rani et al. (2015)), and 0.075 (Joshi et al. [6]), respectively. The coefficient

Table 6
Comparison of average coefficient of friction of the lubricant samples tested in this study.

Description	SAE 15W-40	Biol10	Biol20	Biol30	Biol40	Biol50	Biol100
Average coefficient of friction	0.1501	0.1091	0.0975	0.0803	0.0788	0.071	0.0811
Experimental conditions of the four-ball tribotester	load: 40 kg, rotational speed: 1200 rpm, temperature: 75 °C, duration: 3600 s						

of friction is a crucial tribological characteristic as it indicates the capability of the lubricant to reduce friction between moving components more effectively, potentially improving engine efficiency and reducing wear (Khadem et al. 2024). Based on the results obtained in this study, the coefficients of friction all of the lubricant samples were significantly lower than that of the SAE 15-W40 commercial synthetic lubricant. The UCOCI biolubricant can work as an auxiliary additive to commercial lubricants for lubricating purposes. Most vegetable oils are composed of triglycerides, which are polar ester molecules by nature. The triglyceride chains enhance the biolubricant layer, resulting in increased strength and reduced friction compared with petroleum-derived lubricants. The triglyceride component principally accounts for the low oxidation stability of vegetable oils [57,58]. The UCOCI biolubricant reduces friction between the sliding surfaces owing to the presence of free fatty acids [21]. Non-edible oils have higher acidity due to their higher free fatty acid content, which reduces the coefficient of friction and wear [59].

The significant concentration of unsaturated fatty acids in the UCOCI biolubricant reduces friction due to its high oleic acid content. Fatty acids possess carboxylic groups (COOH) that create a polar coating that adheres to the metal surface, which in turn, reduces friction [60].

3.5.2. Wear scar diameter analysis

The high temperature of the lubricant may cause more wear on sliding and metal contact surfaces [61]. Fig. 11 presents the wear scar diameter results for the UCOCI biolubricant and its blends and the SAE 15W-40 commercial synthetic lubricant. The SAE 15W-40 lubricant had an average wear scar diameter of 0.549 mm. Aravind et al. [15] reported that wear scar diameter for commercial lubricants is within the range of 0.51–0.87 mm. The average wear scar diameter of the UCOCI biolubricant (Biol100) was 17.86 % lower than that of the SAE 15W-40 lubricant. The UCOCI biolubricant resulted in the lowest wear scar diameter and showed superior efficacy in safeguarding the metal-to-metal contact surface area. The wear scar diameters of the UCOCI biolubricant blends were smaller than that of the SAE 15W-40 lubricant. The average wear scar diameters for the Biol10, Biol20, Biol30, Biol40, Biol50, and Biol100 lubricants were 0.140, 0.108, 0.104, 0.100, 0.100, and 0.111 mm, respectively.

Gamma oryzanol and tocopherol are natural antioxidants present in biodegradable oils. The surface protection area between metal contacts expands due to the increased chain length of fatty acids, which enhances the absorption of film thickness as the fatty acid chain length increases [61]. The higher degree of unsaturated fatty acids in the oil results in a decrease in wear. The fatty acid composition of biodegradable oil induces oxidative deterioration [62]. UCOCI biolubricant can suspend wear particles by minimizing wear between contact surfaces and maintaining a lubricant coating to minimize metal–surface interactions. Consequently, the UCOCI biolubricant, when combined with synthetic lubricant, exhibits a lower wear scar diameter compared with the SAE 15W-40 lubricant, indicating the lubrication potential of the UCOCI biolubricant.

The micrographs of the wear scars on the surfaces of stationary steel balls when the UCOCI biolubricant and its blends were employed as the lubricating contact fluid (supplementary). It can be observed that there was a larger wear scar size, several grooves, and material transfer for the SAE 15W-40 commercial synthetic lubricant. The use of the UCOCI biolubricant and its blends as the lubricating medium markedly diminished the wear scar and resulted in subtle grooves on the metal surface. Based on the ASTM D4172–94 standard, the UCOCI biolubricant and its blends outperformed the SAE 15W-40 in minimizing wear and friction between two rolling surfaces. Therefore, it can be deduced that the UCOCI biolubricant has great potential as substitute or additive to conventional petroleum-derived lubricants, which will significantly reduce the reliance on fossil fuel-derived lubricants.

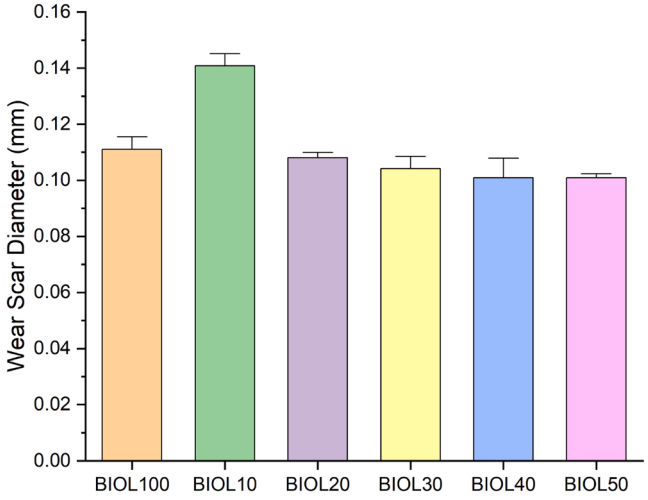

Fig. 11. Average wear scar diameter of the UCOCI of biolubricant and its blends.

4. Conclusion

In this study, UCOCI biolubricant was produced through a two-step transesterification process assisted by infrared irradiation, achieving a maximum conversion rate of 94.30179 % under the following optimal reaction conditions: (1) reaction time: 58.218 min, (2) ratio of EG to UCOCI methyl ester: 23.393 % (v/v), and (3) sodium methoxide catalyst concentration: 0.959 % (w/w). The experimental UCOCI biolubricant yield was found to be 94.0306 %, which showed excellent agreement with the predicted UCOCI biolubricant yield (94.30179 %). The UCOCI biolubricant was evaluated for its physicochemical properties and tribological characteristics using a four-ball tribotester in accordance with the ASTM 4172 standard. The acid value, kinematic viscosities at 40 and 100 °C, VI, flash point, and oxidation stability of the UCOCI biolubricant were 0.46 mg KOH/g, 83.46 and 13.2 cSt, 216.32, 243.3 °C, and 1703.2 min, respectively. The physicochemical properties of the UCOCI biolubricant were close to those specified in the ISO VG 100 standard. The UCOCI biolubricant and its blends demonstrate superior boundary lubrication properties, lower coefficients of friction, and smaller wear scar diameters compared with the SAE 15W-40 commercial synthetic lubricants, indicating their potential as effective heavy-duty engine lubricants and as additives to enhance existing commercial lubricants.

CRediT authorship contribution statement

Bela Nurulita: Writing – original draft, Methodology, Data curation. **Taufiq Bin Nur:** Writing – review & editing, Supervision, Conceptualization. **Arridina Susan Silitonga:** Writing – review & editing, Writing – original draft, Supervision, Funding acquisition, Data curation, Conceptualization. **Teuku Meurah Indra Riayatsyah:** Writing – review

& editing, Writing – original draft, Resources, Methodology, Investigation, Data curation, Conceptualization. **Deswita:** Validation, Methodology. **Md Abul Kalam:** Validation, Supervision. **Nurin Wahidah Mohd Zulkifli:** Supervision, Formal analysis. **Abdi Hanra Sebayang:** Resources. **Sihar Siahaan:** Visualization, Validation. **Munawar Alfansury:** Visualization, Validation.

Declaration of competing interest

The authors declare that they have no known competing financial interests or personal relationships that could have appeared to influence the work reported in this paper.

Acknowledgements

The authors graciously acknowledge the Department of Mechanical Engineering, Universitas Sumatera Utara and University of Technology Sydney (Strategy Research Support Funding 2023 and 2024; 324100.2200035 and 324100.2200144) for funding this study. The authors also wish to thank the Renewable Energy Research Centre and National Innovation and Research Agency (BRIN), Indonesia and Politeknik Negeri Medan (B/159/PL5/PT.01.05/2024) for providing the facilities and tools for testing and analysis.

Supplementary materials

Supplementary material associated with this article can be found, in the online version, at doi:10.1016/j.rineng.2024.103343.

Data availability

The data that has been used is confidential.

References

[1] Energy Institute. Statistical Review of World Energy, 73rd edition, Energy Institute, KEARNEY, 2024.
[2] ESDM, Handbook Of Energy & Economic Statistics Of Indonesia, Kementerian Energi dan Sumber Daya Mineral, 2023.
[3] D. Cao, et al., Biolubricant. Sustainable Production Innovations: Bioremediation and Other Biotechnologies, 2024, pp. 1–56.
[4] K. Chowdary, et al., A review of the tribological and thermophysical mechanisms of bio-lubricants based nanomaterials in automotive applications, J. Mol. Liq. 339 (2021) 116717.
[5] M. Gul, et al., RSM and Artificial Neural Networking based production optimization of sustainable Cotton bio-lubricant and evaluation of its lubricity & tribological properties, Energy Reports 7 (2021) 830–839.
[6] J.R. Joshi, et al., Chemical modification of waste cooking oil for the biolubricant production through transesterification process, J. Indian Chem. Soc. 100 (3) (2023) 100909.
[7] Research, G.V. Grand View Research Market Trend. 2024 Available from: https://www.grandviewresearch.com/market-trends/lubricant-industry-trends.
[8] S. Thapar, Energy and Climate Change. Renewable Energy: Policies, Project Management and Economics: Wind and Solar Power (India), Springer, 2024, pp. 1–11.
[9] S. Shankar, et al., Experimental studies on viscosity, thermal and tribological properties of vegetable oil (kapok oil) with boric acid as an additive, Micro Nano Lett 16 (5) (2021) 290–298.
[10] N. Mohamed, et al., Analysis of the Biodegradable Lubricant in Internal Combustion Engine, Journal of Automotive Powertrain and Transportation Technology 2 (1) (2022) 47–55.
[11] M. Perera, et al., Bioprocess development for biolubricant production using non-edible oils, agro-industrial byproducts and wastes, J Clean Prod 357 (2022) 131956.
[12] R.S. Negi, et al., Potential valorization of used cooking oil into novel biolubricating grease through chemical modification and its performance evaluation, Ind. Crops Prod. 205 (2023) 117555.
[13] M. Zaid, et al., Development of the Calophyllum inophyllum based biolubricant and their tribological analysis at different conditions, Mater. Today: Proc. 26 (2020) 2582–2585.
[14] L.I. Farfan-Cabrera, E.A. Gallardo-Hernández, J. Pérez-González, Compatibility study of common sealing elastomers with a biolubricant (Jatropha oil), Tribol. Int. 116 (2017) 1–8.
[15] A. Aravind, M. Joy, K.P. Nair, Lubricant properties of biodegradable rubber tree seed (Hevea brasiliensis Muell. Arg) oil, Ind. Crops Prod. 74 (2015) 14–19.
[16] A. Silitonga, et al., Intensification of Reutealis trisperma biodiesel production using infrared radiation: simulation, optimisation and validation, Renew Energy 133 (2019) 520–527.
[17] E. Wang, et al., Synthesis and oxidative stability of trimethylolpropane fatty acid triester as a biolubricant base oil from waste cooking oil, Biomass Bioenergy 66 (2014) 371–378.
[18] S. Gupta, et al., Effect of Jojoba oil based biolubricant additive on the friction and wear characteristics of the Al-7Si alloy, Mater. Today: Proc. 26 (2020) 2681–2684.
[19] imarcgroup. Used Cooking Oil Market Report by Source (Household Sector, Commercial Sector), Application (Biodiesel, Oleo Chemicals, Animal feed, and Others), and Region 2024-2032. 2024; Available from: https://www.imarcgroup.com/used-cooking-oil-market.
[20] S. Almasi, et al., A review on bio-lubricant production from non-edible oil-bearing biomass resources in Iran: recent progress and perspectives, J Clean Prod 290 (2021) 125830.
[21] J. Milano, et al., Optimization of biodiesel production by microwave irradiation-assisted transesterification for waste cooking oil-Calophyllum inophyllum oil via response surface methodology, Energy Convers. Manage. 158 (2018) 400–415.
[22] S.K. Kurre, J. Yadav, A review on bio-based feedstock, synthesis, and chemical modification to enhance tribological properties of biolubricants, Ind. Crops Prod. 193 (2023) 116122.
[23] P. Prasannakumar, et al., A comparative study on the lubricant properties of chemically modified Calophyllum inophyllum oils for bio-lubricant applications, J Clean Prod 339 (2022) 130733.
[24] U. Ahmad, et al., Biolubricant production from castor oil using iron oxide nanoparticles as an additive: experimental, modelling and tribological assessment, Fuel 324 (2022) 124565.
[25] N.A. Mohamad Aziz, et al., Prospects and challenges of microwave-combined technology for biodiesel and biolubricant production through a transesterification: a review, Molecules 26 (4) (2021) 788.
[26] K. Rokni, et al., Microwave-assisted synthesis of trimethylolpropane triester (biolubricant) from camelina oil, Sci. Rep. 12 (1) (2022) 11941.
[27] P. San Kong, et al., Enhanced microwave catalytic-esterification of industrial grade glycerol over Brønsted-based methane sulfonic acid in production of biolubricant, Process Saf. Environ. Prot. 104 (2016) 323–333.
[28] S. Almasi, et al., A novel approach for bio-lubricant production from rapeseed oil-based biodiesel using ultrasound irradiation: multi-objective optimization, Sustainable Energy Technol. Assessm 43 (2021) 100960.
[29] N.A. Patience, et al., Ultrasonic intensification to produce diester biolubricants, Ind. Eng. Chem. Res. 58 (19) (2019) 7957–7963.
[30] M. Sanchez, et al., Structural elucidation of complex polyesters polyols from biolubricant using off-line liquid chromatography x supercritical fluid chromatography coupled with Orbitrap mass spectrometry, Talanta 276 (2024) 126295.
[31] W.N. Wulandari, M. Darsin, R.K.K. Wibowo, Study on characteristics of calophyllum inophyllum oil as a new alternative cutting fluid, in: AIP Conference Proceedings, AIP Publishing, 2020.
[32] M. Bahadi, J. Salimon, D. Derawi, Synthesis of di-trimethylolpropane tetraester-based biolubricant from Elaeis guineensis kernel oil via homogeneous acid-catalyzed transesterification, Renew Energy 171 (2021) 981–993.
[33] B. Kamyab, et al., Synthesis of TMP esters as a biolubricant from canola oil via a two-step transesterification–transesterification process, Can. J. Chem. Eng. 102 (1) (2024) 35–52.
[34] A. Ruggiero, et al., Tribological characterization of vegetal lubricants: comparative experimental investigation on Jatropha curcas L. oil, Rapeseed Methyl Ester oil, Hydrotreated Rapeseed oil, Tribol. Int. 109 (2017) 529–540.
[35] J. Milano, et al., Synthesis of Ceiba pentandra biodiesel using ultrasound and infrared radiation: comparison and fuel characterisation, in: IOP Conference Series: Earth and Environmental Science, IOP Publishing, 2024.
[36] P. Selvakumar, P. Sivashanmugam, Ultrasound assisted oleaginous yeast lipid extraction and garbage lipase catalyzed transesterification for enhanced biodiesel production, Energy Convers. Manage. 179 (2019) 141–151.
[37] S. Arumugam, G. Sriram, R. Ellappan, Bio-lubricant-biodiesel combination of rapeseed oil: an experimental investigation on engine oil tribology, performance, and emissions of variable compression engine, Energy 72 (2014) 618–627.
[38] N. Prajapati, et al., Microwave assisted biodiesel production: assessment of optimization via RSM techniques, Mater. Today: Proc. 57 (2022) 1637–1644.
[39] C.N. Ude, et al., Optimization of dual transesterification of jatropha seed oil to biolubricant using hybridized response surface methodology (RSM) and adaptive neuro fuzzy inference system (ANFIS)-genetic algorithm (GA), Sustainable Chem. Environm. 4 (2023) 100050.
[40] S. Hisham, et al., Waste cooking oil blended with the engine oil for reduction of friction and wear on piston skirt, Fuel 205 (2017) 247–261.
[41] N.D. Mu'azu, O. Alagha, I. Anil, Systematic modeling of municipal wastewater activated sludge process and treatment plant capacity analysis using GPS-X, Sustainability 12 (19) (2020) 8182.
[42] F.O. Ifeanyi-Nze, E.T. Akhiehiero, Optimization of the process variables on biodegradable industrial lubricant basestock synthesis from Jatropha curcas seed oil via response surface methodology, Frontiers in Energy Research 11 (2023) 1169565.
[43] N. Zainal, et al., A review on the chemistry, production, and technological potential of bio-based lubricants, Renewable Sustainable Energy Rev. 82 (2018) 80–102.
[44] K.Y. Nandiwale, S.K. Yadava, V.V. Bokade, Production of octyl levulinate biolubricant over modified H-ZSM-5: optimization by response surface methodology, Journal of Energy Chemistry 23 (4) (2014) 535–541.

[45] J. Milano, et al., Tribological study on the biodiesel produced from waste cooking oil, waste cooking oil blend with Calophyllum inophyllum and its diesel blends on lubricant oil, Energy Reports 8 (2022) 1578–1590.
[46] M. Kalam, et al., Influences of thermal stability, and lubrication performance of biodegradable oil as an engine oil for improving the efficiency of heavy duty diesel engine, Fuel 196 (2017) 36–46.
[47] H. Faraj, et al., Optimization of an electrocoagulation-assisted adsorption treatment system for dairy wastewater, Case Studies in Chemical and Environmental Engineering 9 (2024) 100574.
[48] Mohammed, I.S., et al., Synthesis and optimization process of ethylene glycol-based bio-lubricant from palm kernel oil (PKO). 2019.
[49] A.D. de Oliveira, et al., Comprehensive near infrared study of Jatropha oil esterification with ethanol for biodiesel production, Spectrochim. Acta Part A 170 (2017) 56–64.
[50] O. Ocholi, et al., Optimization of the operating parameters for the extractive synthesis of biolubricant from sesame seed oil via response surface methodology, Egypt. J. Pet. 27 (3) (2018) 265–275.
[51] R. Chakraborty, H. Sahu, Intensification of biodiesel production from waste goat tallow using infrared radiation: process evaluation through response surface methodology and artificial neural network, Appl. Energy 114 (2014) 827–836.
[52] A. Bapat, S. Pradhan, C.S. Madankar, Oil and Fats as Raw Materials as Corrosion Inhibitors and Biolubricants, Oils and Fats as Raw Mater. Industry (2024) 195–229.
[53] G. Appiah, et al., Biolubricant production via esterification and transesterification processes: current updates and perspectives, Int. J. Energy Res. 46 (4) (2022) 3860–3890.
[54] Crown, O., Fuels and lubricants -hydraulic fluids. 2023, https://www.crownoil.co.uk/guides/hydraulic-oil-guide/.
[55] A. Paar, ISO Viscosity Classification 3448 (2023).
[56] D. Kania, et al., A review of biolubricants in drilling fluids: recent research, performance, and applications, J. Pet. Sci. Eng. 135 (2015) 177–184.
[57] X. Zhang, et al., Vegetable oil-based nanolubricants in machining: from physicochemical properties to application, Chinese J. Mech. Eng. 36 (1) (2023) 76.
[58] R. Al Sulaimi, et al., Evaluating the effects of very long chain and hydroxy fatty acid content on tribological performance and thermal oxidation behavior of plant-based lubricants, Tribol. Int. 185 (2023) 108576.
[59] M.A. Jumaah, et al., Synthesis of tri, tetra, and hexa-palmitate polyol esters from Malaysian saturated palm fatty acid distillate for biolubricant production, Biomass Conversion and Biorefinery 14 (2) (2024) 1919–1937.
[60] K. Yoshida, Y. Naganuma, M. Kano, Effect of degree of unsaturation in vegetable oils on friction properties of dlc coatings, Tribology Online 16 (4) (2021) 210–215.
[61] J. Tian, et al., Friction behaviors and wear mechanisms of multi-filler reinforced epoxy composites under dry and wet conditions: effects of loads, sliding speeds, temperatures, water lubrication, Tribol. Int. 179 (2023) 108148.
[62] M.M.F. Melo Neta, et al., Thermo-oxidative stability and tribological properties of biolubricants obtained from castor oil fatty acids and isoamyl alcohol, Lubricants 11 (11) (2023) 490.